Processing and Application of Ceramics 16 [4] (2022) 367–373
https://doi.org/10.2298/PAC2204367U

Room temperature plasticity of zirconia-yttria-titania ceramics: Experimental indications and structural modelling

Valter Ussui†[1], Dolores Ribeiro Ricci Lazar[1,*], Nelson Batista de Lima[1], Anelyse Arata[1,2], Fabio Negreiros Ribeiro[1], Gustavo Martini Dalpian[1,2], Juliana Marchi[1], José Octavio Armani Paschoal[1,2]

[1]*Instituto de Pesquisas Energéticas e Nucleares (IPEN/CNEN), Av. Prof. Lineu Prestes, 2242 - Cidade Universitária, CEP 05508-000, São Paulo, Brazil*
[2]*Centro de Ciências Naturais e Humanas (CCNH), Universidade Federal do ABC (UFABC), Av. dos Estados, 5001 - CEP 09210-580, Santo André, São Paulo, Brazil*
[3]*INFIQC, CONICET, Departamento de Química Teórica y Computacional, Facultad de Ciencias Químicas, Universidad Nacional de Córdoba, Av. Medina Allende y Haya de la Torre, X5000 HUA, Córdoba, Argentina*
[4]*Instituto de Astronomia, Geofísica e Ciências Atmosféricas da Universidade de São Paulo (IAG-USP), R. do Matão, 1226 - Cidade Universitária, CEP 05508-090, São Paulo, Brazil*

Received 18 May 2022; Received in revised form 9 September 2022; Accepted 21 October 2022

Abstract

Yttria-stabilized tetragonal zirconia (Y-TZP) ceramics have excellent mechanical properties. However, such materials cannot undergo plastic deformation at room temperature due to their high hardness and brittleness values, hindering machinability. To overcome these limitations, we propose a zirconia-yttria-titania ceramics, based on zirconia containing 3 mol% yttria and up to 15 mol% titania. The zirconia-yttria-titania powders were synthesized by co-precipitation method, uniaxially pressed and sintered at 1400 °C/5 h. Sample characterizations were carried out by X-ray diffraction, scanning electron microscopy and mechanical properties through Vickers hardness and toughness measurements. Compared to the Y-TZP ceramics, the yttria stabilised tetragonal zirconia ceramics co-doped with 10 mol% Ti showed noticeable increase of tetragonality parameter, higher toughness and lower hardness values, indicating plasticity at room temperature. Furthermore, the atomistic simulation by Density Functional Theory methodology suggests the occurrence of spatial arrangement of the atoms, explaining the proposed plasticity.

Keywords: *zirconia, yttria, titania, density functional theory, plasticity*

I. Introduction

Structural advanced ceramics are known for their general properties, such as high hardness, brittleness, resistance to chemical corrosion and high-temperature mechanical resistance [1]. Despite its good mechanical properties, when a ceramic material suffers a local stress concentration, a brittle fracture can occur with negligible plastic deformation, since dislocations are relatively immobile and dislocation-induced plasticity is almost absent [2]. These characteristics are a consequence of the nature of the chemical bonding between its ions, which has a mixed ionic and covalent character [3]. Plastic deformation is associated with the movement of large number of dislocations, typically found in metallic materials. However, considering materials with high content of ionic bonds, there are few sliding planes where dislocations can move. Sliding systems are also limited in covalent ceramics since this kind of bonding is always relatively strong and highly oriented [2]. In order to promote plastic deformation in a ceramic material, different approaches have been studied, such as high-temperature treatments, where more than 1000% plastic elongation was observed at temperatures higher

*Corresponding author: tel: +55 11 28105594
e-mail: *drlazar@ipen.br*
† This paper is dedicated to the memory of Prof. Valter Ussui who passed away on January 21st, 2021

than 1000 °C [4]. This exceptional elongation in tensile deformation characterizes the superplasticity phenomenon in various polycrystalline solids. Even though several experimental researches consider the superplasticity properties, its mechanism is still not precise. Most researchers reported in the literature emphasize that the superplasticity phenomenon in zirconia based ceramics could only be observed at very high temperatures or with nanoscale particles dimensions [5–8].

The increase of biomedical applications of zirconia ceramics requires the improvement of their machinability to suit the shape and dimensions of sintered specimens. When previously sintered, those systems are very hard to be adequately machined during fabrication [9,10]. In dentistry, it is also important to consider that excessive hardness of an implant or restoration can be detrimental to the masticatory system. In order to minimize this problem, Kim *et al.* [11] developed zirconia ceramics comprising titania nanopowder with decreased hardness, maintaining high strength and fracture toughness. Thus, besides the addition of yttria to zirconia, this behaviour could be achieved by addition of niobia, tantala and titania.

It is well known that two classic mechanisms that explain the enhancement of mechanical properties of zirconia ceramics are: i) microcracking formation due to a controlled tetragonal → monoclinic phase transformation during ceramic processing and ii) stress-induced transformation toughening [12]. After forty years of discovering the stress-induced transformation of metastable tetragonal zirconia by Garvie *et al.* [12], Chevalier *et al.* [13] highlighted that Ce-doped zirconia with alumina and strontium aluminate additions could display a significant amount of transformation-induced plasticity without damage, which is a promising mechanism to allow the use of additive manufacturing processing. Recently, Luo *et al.* [14] synthesized a Y-TZP-TiO_2 composite containing 0–10 mol% TiO_2 by a powder mixing process. The increase in TiO_2 content increased the bending strength and hardness to a certain extent. The wear mechanism of those ceramics was mainly attributed to plastic deformation and microcracking.

In the present study we demonstrate that plastic deformation of zirconia-yttria-titania ceramics, prepared by co-precipitation route, can occur at room temperature, simultaneously with transformation toughening. This behaviour can be achieved under restricted chemical compositions and processing conditions, based on microstructural, hardness and fracture toughness evaluation. This phenomenon is proposed by comparing experimental results with modelling experiments using Density Functional Theory (DFT), considered by far as the most widely used theoretical method to describe an electronic structure [15].

II. Experimental

Zirconia-yttria-titania powders were prepared by co-precipitation method using zirconium oxychloride (IPEN/CNEN, Brazil) and yttrium and titanium chlorides prepared from their metal oxides (Sigma Aldrich, USA and CAAL, Brazil, respectively). The studied compositions contained 3 mol% Y_2O_3 and 0–15 mol% TiO_2. The samples were codified as ZY3T*x*, where *x* is the TiO_2 molar concentration. According to experimental conditions established in our previous work [16], the zirconium oxychloride, titanium chloride and yttrium chloride solutions were mixed and added drop-wise to an aqueous solution of ammonium hydroxide. The obtained precipitates were filtered and washed successively with water and then with ethanol. In order to prevent agglomerate formation, precipitates were treated by azeotropic distillation with n-butyl alcohol. After drying, the powders were calcined at 800 °C and uniaxially pressed into disks with diameter of 10 mm and height of 3.5 mm. Five disks of each composition were prepared. These samples were sintered at 1400 °C in an air atmosphere for 5 h (Lindberg Blue M box furnace, USA).

The crystal structures of the zirconia-yttria-titania ceramic samples were analysed on a Rigaku DMAX 2000 diffractometer, followed by Rietveld refinement (GSAS, USA). These data allowed the determination of phase content and crystal cell parameters. Theoretical density of each sample was determined for two cases: considering and not considering the substitution of Zr^{4+} by Ti^{4+} in the lattice. Densities of the sintered ceramics were measured by immersion method. For each composition, the experimental densities of five samples were measured in order to calculate the mean value and the standard deviation. Relative density (%TD) was calculated from the measured and theoretical density values. Longitudinal sections of the samples were polished with conventional diamond suspensions and Vickers hardness of the disks was evaluated. A Buehler VMT-7 pyramidal indentation (136°) was used with a 200 N load applied perpendicularly to the polished surface of the samples, considering ten measurements for each composition for statistical analysis. After hardness impression tests, the fracture toughness of the disks was calculated using the equation developed by Shetty, Wright, Mincer and Clauer (SWMC equation) which was normalized by Ponton and Rawlings for Palmqvist crack model [17]. Following the Vickers impressions, the microstructures were observed with a Philips XL-30 scanning electron microscope (SEM). The samples were thermally treated at 1350 °C for 30 min (Lindberg Blue M Elevator Hearth furnace) to reveal the grain boundaries. The measurements of the grain size were calculated using the Quantikov software [18].

To better understand the experimental findings, atomistic simulations were performed at the density functional level [19] within the Perdew-Burke-Ernzerhof [20] exchange-correlation functional using the Quantum Espresso (QE) software [21]. The GBRV pseudopotentials [22] were used with the standard plane-wave and charge density cut-offs of 40/200 Ryd, a $2 \times 2 \times 2$

Monkhorst-Pack k-point sampling [23], a 1×10^{-8} a.u. energy threshold for self-consistency and $1 \times 10^{-5}/1 \times 10^{-4}$ a.u. energy/force thresholds for geometry and cell optimizations. A-Basin hopping optimization approach [24] was employed to search for the most stable chemical configurations at each composition. A fictitious temperature of 150 K and an average of 1500 steps were used. More details of the computation approach used can be found elsewhere [23,25].

III. Results and discussion

3.1. Structural characterization

XRD results (Fig. 1a) showed that only zirconia polymorphic phases were identified after sintering but in different crystallographic structures depending on amount of titania (JCPDS cards 50-1089; 89-7710 and 89-9069 for monoclinic, tetragonal and cubic phases, respectively). Cubic phase was present in all samples, with the highest content in the ZY3T5 ceramics containing 5 mol% of titania. This result indicates that, for the studied compositions, the incorporation of Y^{3+} and Ti^{4+} in ZrO_2 structure occurs. This behaviour is expected due to the similarity of Zr^{4+} and dopants ionic radii in eightfold coordination, i.e. stabilization of tetragonal and cubic zirconia symmetry. It is well known that the most suitable dopants for zirconia are those cations whose radius ratio difference is <40%, compared to that of Zr^{4+} [26]. For eightfold coordination this condition is fulfilled, considering that Zr^{4+}, Y^{3+} and Ti^{4+} ionic radii are 0.84 Å, 1.019 Å and 0.74 Å, respectively [27]. Besides that, the zirconia-yttria-titania phase diagram proposed by Schaedler *et al.* [28] shows that the solubility limit of Ti^{4+} in zirconia structure is around 20 mol%. The monoclinic phase was also found in all studied compositions as a secondary phase, including the control 3Y-TZP ceramics. The monoclinic content is maximal when the amount of titania is 10 mol%.

Unit cell parameters (a, c) and the relation c/a of the tetragonal phase are shown in Table 1. For the studied composition it was observed that tetragonality (c/a) increases with titania content, without reaching the solubility limit of tetragonal phase, according to XRD data. The increased tetragonality is an indication of sliding of planes with Ti^{4+} addition in the lattice, occupying Zr^{4+} position [25].

Relative densities of the sintered samples, calculated from the relation between experimental and theoretical densities calculated from Rietveld refinement results, are given in Table 1. After sintering, densification was attained, especially for the samples with lower titania content, reaching relative densities from 92.6 to 99.1 %TD (Table 1 and Fig. 1b). These values were calculated considering theoretical densities without Ti^{4+} in zirconia lattice, indicating that the increase of titania content leads to lower densities. On the other hand,

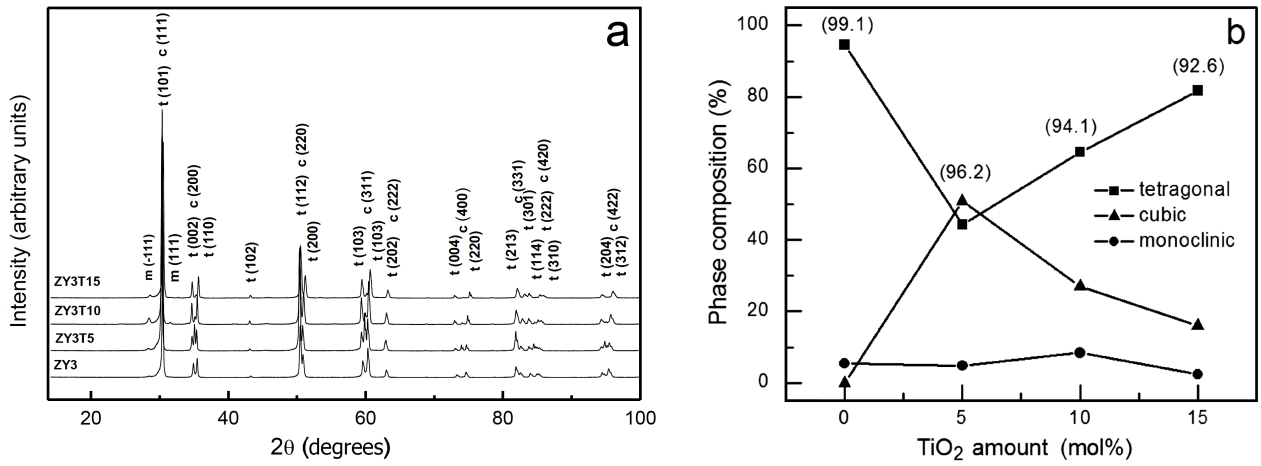

Figure 1. (a) XRD patterns of zirconia-yttria-titania ceramics (m - monoclinic, c - cubic and t - tetragonal phases) and (b) phase composition with corresponding relative density values in parenthesis (theoretical densities were calculated from Rietveld's refinement)

Table 1. Measured (ρ), theoretical (ρ_{th}) and relative (ρ_r) densities, unit cell parameters (a, c) and tetragonality (c/a) determined by Rietveld refinement of XRD data of zirconia-yttria-titania ceramics

Sample	ρ [g/cm^3]	ρ_{th} [g/cm^3]	ρ_r [%TD]	a [Å]	c [Å]	c/a
ZY3	5.99 ± 0.01	6.04	99.1 ± 0.2	3.603	5.1723	1.4355
ZY3T5	5.84 ± 0.01	6.07* (5.97)**	96.2 ± 0.2* 97.8 ± 0.2**	3.5951	5.1819	1.4414
ZY3T10	5.70 ± 0.01	6.06* (5.82)**	94.1 ± 0.2* 97.9 ± 0.2**	3.5877	5.1872	1.4458
ZY3T15	5.65 ± 0.01	6.10* (5.75)**	92.6 ± 0.2* 98.2 ± 0.2**	3.5814	5.1956	1.4507

* Rietveld refinement not considering Ti^{4+} in zirconia lattice

** Rietveld refinement considering Ti^{4+} in zirconia lattice

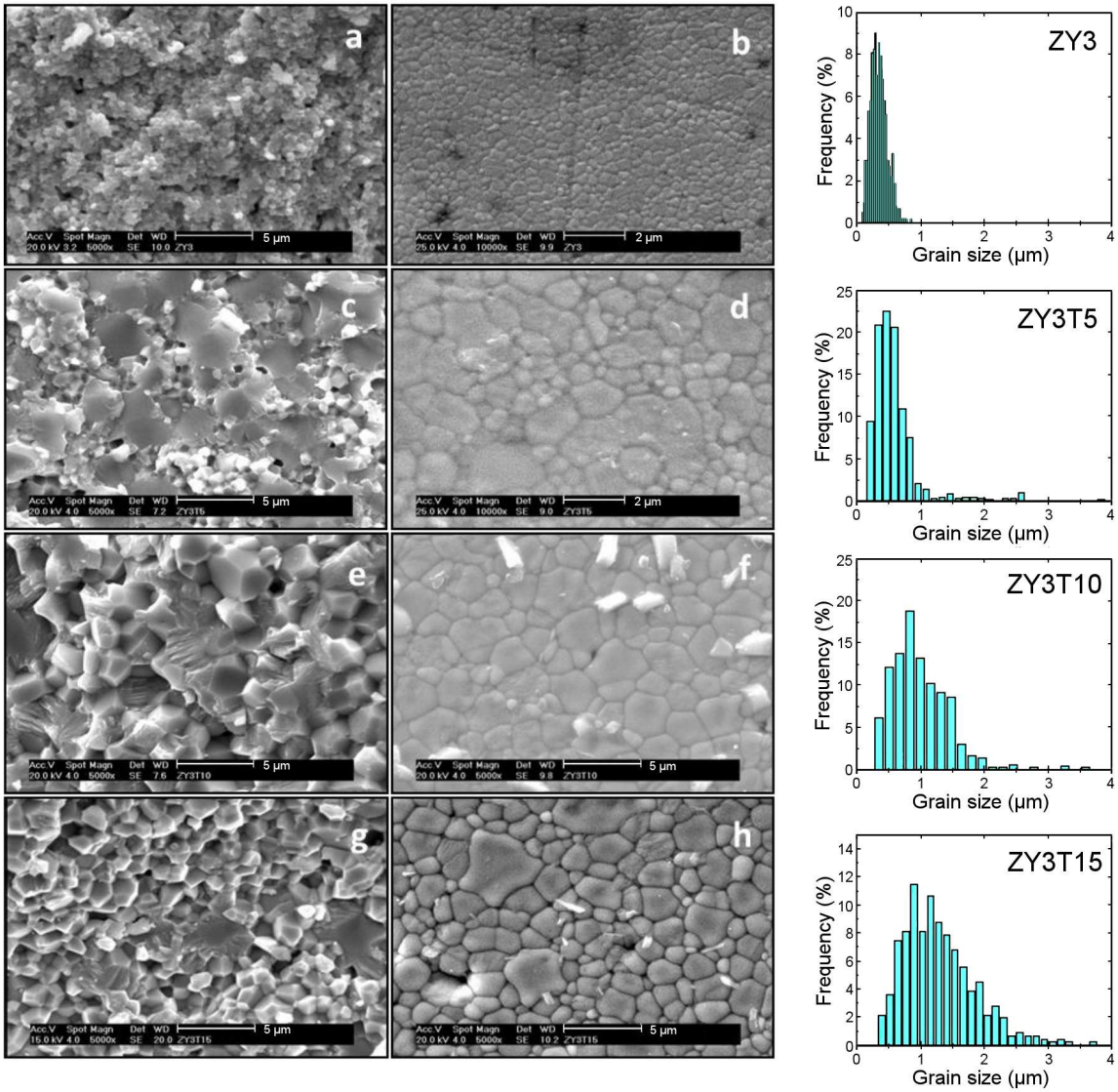

Figure 2. SEM micrographs and grain size distribution of zirconia-yttria-titania ceramics: (a, c, e, g) SEM of the fracture surface; (b, d, f, h) SEM of the polished and thermally etched surfaces and corresponding grain size distribution graphs

relative densities calculated by including Ti^{4+} in zirconia lattice indicated high densification for all titania contents (Table 1), as observed in SEM micrographs (Fig. 2).

Microstructure of the sintered ceramics was observed by SEM on the fractured surfaces and polished and thermally etched surfaces (Fig. 2). An increase in grain size was observed as the titania amount increased in the ceramics. The fracture surface of the Y-TZP sample shows a typical tetragonal zirconia microstructure, with a homogeneous distribution of sub-micrometric grains and only intergranular fracture (Fig. 2a). Fracture surface micrographs of the titania-containing samples (Figs. 2c,e,g) show predominant small tetragonal grains with round shapes, few larger cubic grains with sharp corners and monoclinic twinned grains. After polishing and thermal etching, a small amount of white exposed structures having higher titania concentration were observed (Figs. 2f,h). These grains could be related to the exsolution of titanium-rich titanates ($ZrTiO_4$). However, this compound was not identified by X-ray diffraction probably due to the limit detection of XRD technique (2 wt.%). This outcrop seems to obey some orientation and results from the stress relief related to the local titanium concentration [29,30].

3.2. Mechanical properties

Mechanical properties were estimated from hardness and fracture values through Vickers indentation methodology. Higher amounts of titania in the studied ceramics lead to the linear decrease of the hardness (Fig. 3a). However, fracture toughness increased in the samples containing up to 10 mol% of titania, reaching unusually high values compared to the control Y-TZP (Fig. 3b). The amount of titania directly affects the grain size and mechanical properties of the zirconia-yttria-titania ceramics. SEM images of the Y-TZP sample (Fig. 3c) revealed a homogeneous grain-size distribution and the crack propagated by an intergranular fracture mode. For the ceramics containing 5 mol% of tita-

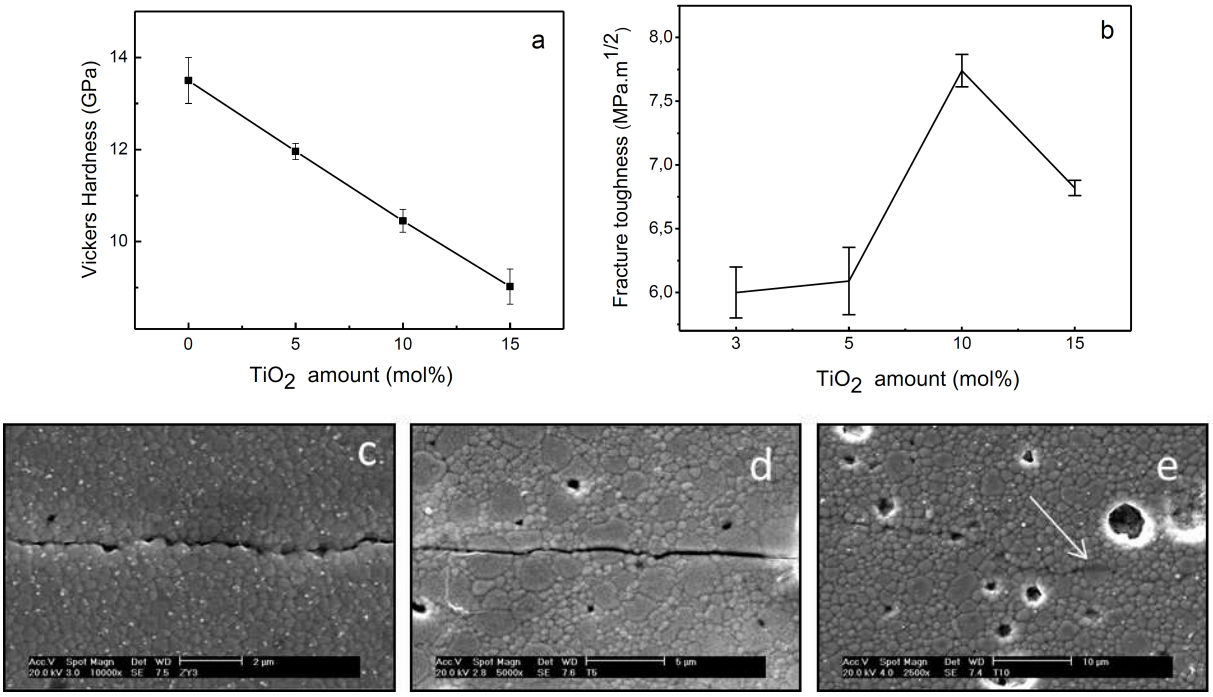

Figure 3. Mechanical properties of zirconia-yttria-titania ceramics as a function of titania content: a) Vickers hardness and b) fracture toughness. SEM micrographs of cracks generated after Vickers indentation test: c) Y-TZP, d) ZY3T5 and e) ZY3T10 (arrow indicates deformed grain)

nia (Fig. 3d), a bimodal grain size distribution was observed and cracks propagation with intergranular fracture mode for smaller grains, and deflection of crack propagation direction and intragranular mode for larger grains. In the last case (the ZY3T10 sample), the direction of the crack propagation was maintained (Fig. 3e). Due to the more cubic phase (>50 wt.%) presented in the sample ZY3T5, the lower fracture toughness values can be attributed to the higher amount of energy dissipated to fracture large grains. For the sample containing 10 mol% of titania (Fig. 3e), intergranular fracture mode is predominant, with a secondary intragranular fracture mode. In this ceramics, crystal structure is mainly tetragonal (64 wt.%), even for larger grains. It is also observed that larger grains can be deformed but not fractured (see arrow in Fig. 3e), suggesting a ductile behaviour. The ZY3T15 sample showed lower fracture toughness than the ZY3T10 ceramics. This behaviour may be due to larger grain size of the ZY3T15 ceramics, even though the tetragonal phase concentration is higher and could allow the transformation toughening mechanism.

3.3. DFT calculations

DFT simulation of the tetragonal 3 mol%-yttria stabilised zirconia used a $2 \times 2 \times 2$ supercell containing 32 ZrO_2 units, one Y_2O_3 unit and one oxygen vacancy to keep charge neutrality. The most stable position of two Y atoms was optimized and found it to be the second neighbour of the oxygen vacancy and the third neighbour to each other, as illustrated in Fig. 4a, being in agreement with the literature [31–33]. The addition of titania was analysed by direct substitution of Zr with Ti atoms, varying the Ti concentration from 3 to 19 mol%. The most stable sites for the substitutional Ti atom were determined using a Basin Hopping global optimization approach that generated a set of hundreds of different chemical arrangements. The most stable chemical configurations found are illustrated in Figs. 4b-d, for the 3, 12, and 19 mol% Ti, respectively. For Ti concentrations up to 9 mol%, the most stable sites were found to maximize the interaction between the added Ti and the oxygen vacancy, which can be understood given the lower Ti coordination and Ti–O bond distances in anatase/rutile phases, so the doped Ti atom close to the oxygen vacancy gives a better strain release. For the composition with 12 mol% of Ti, the added Ti forms an infinite channel in the [100] or [010] directions, always tangent to the oxygen vacancy and between mixed Y-Zr rows. Further addition of Ti increases the size of the channel, up to the formation of an almost complete TiO_2 plane parallel to the longer *c* axis at Ti concentration of 19 mol%.

To estimate how these channels change the material's response to dislocations, the energy needed to slide a single plane composed of mixed Zr/Ti cations was evaluated for different Ti compositions (Fig. 4e). In this calculation, one (100) plane is displaced in the [010] direction from 0–0.5 nm, in steps of 0.001 nm. At each step, all atoms and coordinates are allowed to relax, accept the *y*-coordinate of the plane being translated (illustrated by a magenta box in Fig. 4e) and the farthest parallel plane (illustrated by a red box in Fig. 4e). The result is shown in Fig. 4f, where a minimal reduction

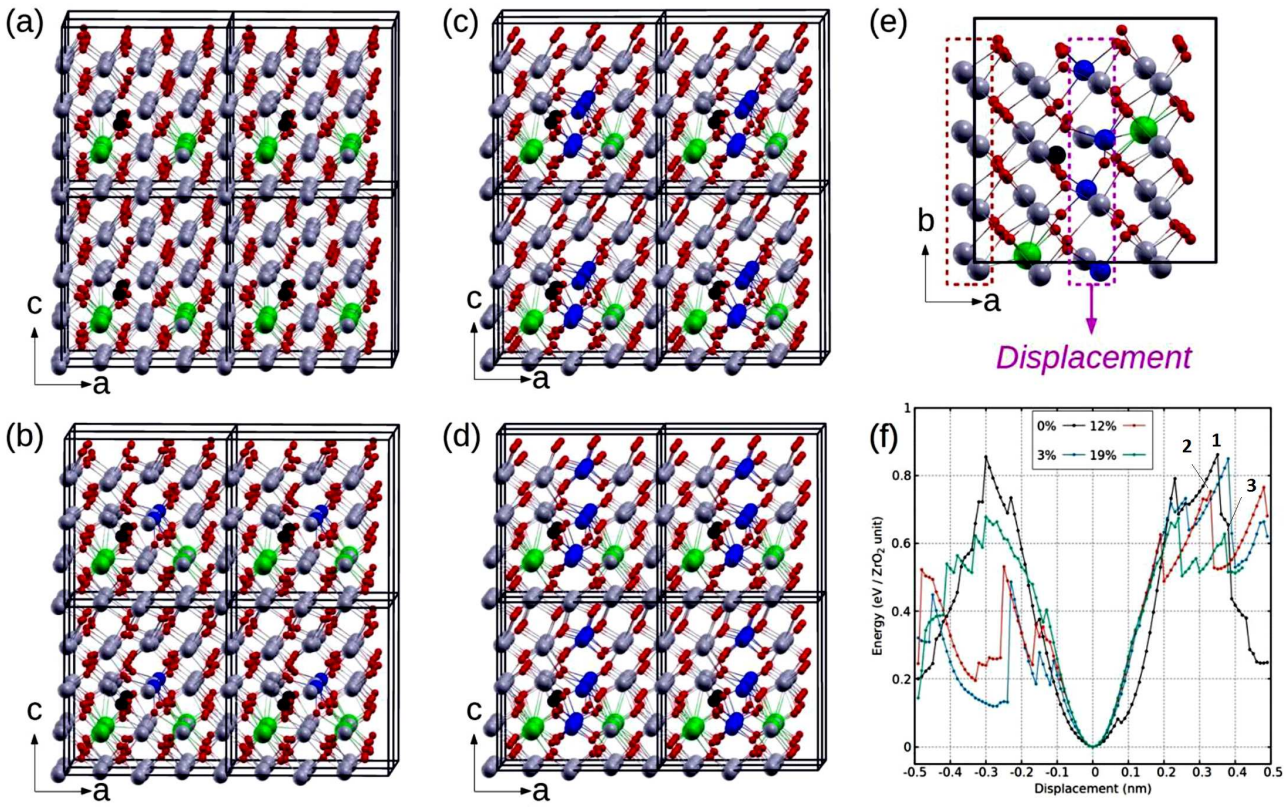

Figure 4. Side view of the tetragonal 2 × 2 × 2 supercell (doubly reproduced in every direction) for the 3 mol%-ytria stabilised zirconia (a) and corresponding side view for the structures with: b) 3 mol%, c) 12 mol% and d) 19 mol% of Ti (Zr/O/Y/Ti atoms are in gray/red/green/blue colour and the vacancy is represented with a dark black sphere). Top view of the structure with 12 mol% Ti, highlighting the sliding plane (magenta dashed rectangle) and the plane in which the *y*-axis of each atom is kept frozen (red dashed rectangle) during the reoptimization. Energy change with displacement (f) confirms that the energy increase is due to the sliding (illustrated in Fig. e) for each of the Ti compositions considered.

of 0.01 eV per ZrO_2 unit for the structure with 3 mol% doping concentration was observed. However, the structures with 12 and 19 mol% Ti presented a much more significant reduction of 0.11 and 0.19 eV, respectively. These values were obtained by the energy difference between structures without Ti and with Ti at the displacement in the range of 0.33–0.38 nm, as pointed out in Fig. 4f (numbers 1, 2 and 3).This result agrees with the experimental hypothesis that the formation of titania channels inside the structure facilitates the strain release between planes, increasing its overall resistance to fracture.

Based on the DFT modelling and experimental results, it was proposed that the increase in toughness values is caused by the selective distribution of Ti atoms in the Y-TZP solid solution. These oriented Ti zones form Ti-rich phase that acts as dislocations and consequently lead to the sliding planes, altering the mechanical behaviour of the ceramics.

IV. Conclusions

In summary, the co-precipitation method allowed the synthesis of chemically homogeneous 3 mol% yttria stabilised tetragonal zirconia powders co-doped with up to 15 mol% of Ti. After sintering at 1400 °C, the dense ceramics were formed containing mainly a mixture of tetragonal and cubic phases. Larger grain sizes in the Ti-doped ceramics compared to the Y-TZP ceramics were observed. Vickers hardness decreases with the addition of titania while fracture toughness is improved, reaching a maximum value at 10 mol% of Ti. This content corresponds to a mixture of tetragonal and cubic phase, with a minor concentration of monoclinic phase. For this composition an intergranular fracture is also observed next to tetragonal grains (characteristic of transformation toughening mechanism) and deformation of large cubic phase grains. The DFT atomistic simulation confirms that when Ti concentration is up to 9 mol%, titanium atom is close to oxygen vacancy resulting in a better strain release.

Acknowledgements: The authors acknowledge the Microscopy laboratory group of the Materials Science and Technology Center (CECTM - IPEN), especially Nildemar A.M. Ferreira, Celso V. de Morais, and Dr. Ana Helena Bressiani, for their helpful technical contribution. The authors are also grateful to Coordination for the Improvement of Higher Education Personnel (PNPD/CAPES, Brazil) for the postdoctoral scholarship granted to Dr. Anelyse Arata and the São Paulo Research Foundation (Fapesp, #14271-9/2014) for the

postdoctoral scholarship granted to Dr. Fábio Negreiros Ribeiro. GMD thanks financial support from FAPESP and CNPq. *Ab initio* calculations were performed at the Santos Dumont Supercomputer at LNCC/Brazil.

References

1. W.D. Kingery, H.K. Bowen, D.R. Uhlmann, *Introduction to Ceramics*, John Wiley & Sons, New York, 1976.
2. R. Danzer, T. Lube, P. Supancic, R. Damani, "Fracture of Ceramics", *Adv. Eng. Mater.*, **10** (2008) 275–298.
3. W.D. Callister Jr., D.G. Rethwisch, *Materials Science and Engineering: An Introduction*; John Wiley & Sons, New York, 2002.
4. F. Wakai, "Superplasticity of ceramics", *Ceram. Int.,* **17** (1991) 153–163.
5. S. Tekeli, T. Chen, H. Nagayama, T. Sakuma, M.L. Mecartney, "High-temperature deformation behaviour of TiO_2-doped 8 mol.% Y_2O_3-stabilized ZrO_2 (8Y-CSZ) under tension and compression", *Ceram. Int.,* **33** (2007) 869–874.
6. E. Camposilvan, M. Anglada, "Size and plasticity effects in zirconia micropillars compression", *Acta Mater.*, **103** (2016) 882–892.
7. Z. Du, X.M. Zeng, Q. Liu, A. Lai, S. Amini, A. Miserez, C.A. Schuh, C.L. Gan, "Size effects and shape memory properties in ZrO_2 ceramic micro- and nano-pillars", *Scr. Mater.,* **101** (2015) 40–43.
8. X.M. Zeng, Z. Du, C.A. Schuh, N. Tamura, C.L. Gan, "Microstructure, crystallization and shape memory behavior of titania and yttria co-doped zirconia", *J. Eur. Ceram. Soc.,* **36** (2016) 1277–1283.
9. I. Denry, J. Kelly, "State of the art of zirconia for dental applications", *Dent. Mater.*, **24** (2008) 299–307.
10. E.D. Rekow, N.R.F.A. Silva, P.G. Coelho, Y. Zhang, P. Guess, V.P. Thompson, "Performance of dental ceramics: Challenges for improvements", *J. Dent. Res.*, **90** (2011) 937–952.
11. S.W. Seo, Y.H. Jeong, D.-J Kim, S.W. Kim, "Machinable zirconia comprising titania nanopowder", US Patent 9,545,363 B2, January, 2017.
12. R.C. Garvie, R.H. Hannik, R.T. Pascoe, "Ceramic steel?", *Nature*, **258** (1975) 703–704.
13. J. Chevalier, A. Liens, H. Reveron, F. Zhang, P. Reynaud, T. Douillard, L. Preiss, V. Sergo, V. Lughi, M. Swain, N. Courtois, "Forty years after the promise of ceramic steel?: Zirconia-based composites with a metal-like mechanical behavior", *J. Am. Ceram. Soc.,* **103** (2020) 1482–1513.
14. P. Luo, J. Zhang, Z. You, X. Ran, Y. Liu, S. Li, S. Li, "Effect of TiO_2 content on the microstructure and mechanical and wear properties of yttria-stabilized zirconia ceramics prepared by pressureless sintering", *Mater. Res. Express*, **6** (2020) 125211.
15. T. van Mourik, M. Bühl, M.-P. Gaigeot, "Density functional theory across chemistry, physics and biology Introduction", *Philos. Trans. R. Soc. A Math. Phys. Eng. Sci.,* **372** (2014) 20120488.
16. V. Ussui, F. Leitão, C. Yamagata, C.A.B. Menezes, D.R. R. Lazar, J.O.A. Paschoal, "Synthesis of ZrO_2-based ceramics for applications in SOFC", *Mater. Sci. Forum,* **416-418** (2003) 681–687.
17. C.B. Ponton, R.D. Rawlings, "Vickers indentation fracture toughness test Part 1 Review of literature and formulation of standardised indentation toughness equations", *Mater. Sci. Technol.,* **5** (1989) 865–872.
18. L.C.M. Pinto, V. Vasconcelos, W.L. Vasconcelos, J.C. Bressiani, "An algorithm of digital image processing applied to quantification of grains with discontinuous boundaries", *Acta Microsc.,* **5** (1996) 168–169.
19. P. Hohenberg, W. Kohn, "Inhomogeneous electron gas", *Phys. Rev.,* **136** (1964) B864.
20. J.P. Perdew, K. Burke, M. Ernzerhof, "Generalized gradient approximation made simple", *Phys. Rev. Lett.,* **77** (1996) 3865–3868.
21. P. Giannozzi, S. Baroni, N. Bonini, M. Calandra, R. Car, C. Cavazzoni, D. Ceresoli, G.L. Chiarotti, M. Cococcioni, I. Dabo, A. Dal Corso, S. de Gironcoli, S. Fabris, G. Fratesi, R. Gebauer, U. Gerstmann, C. Gougoussis, A. Kokalj, M. Lazzeri, L. Martin-Samos, N. Marzari, F. Mauri, R. Mazzarello, S. Paolini, A. Pasquarello, L. Paulatto, C. Sbraccia, S. Scandolo, G. Sclauzero, A.P. Seitsonen, A. Smogunov, P. Umari, R. M. Wentzcovitch, "Quantum Espresso: A modular and open-source software project for quantum simulations of materials", *J. Phys. Condens. Matter.*, **21** (2009) 395502.
22. K.F. Garrity, J.W. Bennett, K.M. Rabe, D. Vanderbilt, "Pseudopotentials for high-throughput DFT calculations", *Comput. Mater. Sci.,* **81** (2014) 446–452.
23. H.J. Monkhorst, J.D. Pack, "Special points for Brillouin-zone integrations", *Phys. Rev. B,* **13** (1976) 5188–5192.
24. D.J. Wales, H.A. Scheraga, "Global optimization of clusters, crystals, and biomolecules", *Science*, **285** (1999) 1368–1372.
25. N. Ribeiro, D.R.R. Lazar, V. Ussui, N.B. de Lima, J. Marchi, G.M. Dalpian, "*Ab initio* atomistic description of temperature-induced phase changes: The cases of zirconia and Ti-Y-co-doped zirconia", *Phys. Rev. Materials*, **5** (2021) 023603.
26. D.J. Green, R.H.J. Hannink, M.V. Swain, *Transformation Toughening of Ceramics*, CRC, Boca Raton,1989.
27. R.D. Shannon, "Revised effective ionic radii and systematic studies of interatomic distances in halides and chalcogenides", *Acta Cryst.*, **A32** (1976) 751–767.
28. T.A. Schaedler, O. Fabrichnaya, C.G. Levi, "Phase equilibria in the TiO_2-$YO_{1.5}$-ZrO_2 system", *J. Eur. Ceram. Soc.*, **28** (2008) 2509–2520.
29. E. McHale, R.S. Roth, "Low-temperature phase relationships in the system ZrO_2-TiO_2", *J. Am. Ceram. Soc.*, **69** (1986) 827–832.
30. F. Azough, R. Freer, J. Petzelt, "A Raman spectral characterization of ceramics in the system ZrO_2-TiO_2", *J. Mater. Sci.,* **28** (1993) 2273–2276.
31. H. Ding, A.V. Virkar, F. Liu, "Defect configuration and phase stability of cubic versus tetragonal yttria-stabilized zirconia", *Solid State Ionics,* **215** (2012) 16–23.
32. A. Predith, G. Ceder, C. Wolverton, K. Persson, T. Mueller, "*Ab initio* prediction of ordered ground-state structures in ZrO_2-Y_2O_3", *Phys. Rev. B - Condens. Matter Mater. Phys.*, **77** (2008) 144104.
33. D. Sangalli, A. Debernardi, "Exchange-correlation effects in the monoclinic to tetragonal phase stabilization of yttrium-doped ZrO_2: A first-principles approach", *Phys. Rev. B*, **84** (2011) 214113.